

See discussions, stats, and author profiles for this publication at: <https://www.researchgate.net/publication/236880044>

ChemInform Abstract: Vibrational Spectroscopy of Bulk and Supported Manganese Oxides.

ARTICLE *in* PHYSICAL CHEMISTRY CHEMICAL PHYSICS · MARCH 1999

Impact Factor: 4.49 · DOI: 10.1039/a807821a

CITATIONS

186

READS

120

4 AUTHORS, INCLUDING:



Dietrich R. T. Zahn

Technische Universität Chemnitz

775 PUBLICATIONS 6,425 CITATIONS

[SEE PROFILE](#)

Vibrational spectroscopy of bulk and supported manganese oxides

Florina Buciuman,*† Florin Patcas,† Radu Craciun† and Dietrich R. T. Zahn

Institut für Physik, Technische Universität Chemnitz, D-09107 Chemnitz, Germany

Accepted and transferred from *Berichte, Bunsen-Gesellschaft* 7th October 1998



Manganese oxide catalysts, both bulk and supported on $\gamma\text{-Al}_2\text{O}_3$ and SiO_2 , have been studied by Raman and FTIR spectroscopies, their phase composition being determined by X-ray diffraction. The supported catalysts were prepared via pore volume impregnation from nitrate precursors, the atomic ratio of manganese to aluminium and silicon, respectively, being in the range from 0.5/100 to 18/100. The use of Raman analysis in the microscopic configuration allowed the spectra to be taken at different points of the surface and revealed the inhomogeneity of the catalyst. Besides the Raman features of the $\beta\text{-MnO}_2$ and $\alpha\text{-Mn}_2\text{O}_3$ phases, other signals were assigned to isolated Mn^{2+} ions accommodated in tetrahedral vacancies on the support surface and to some epitaxial layers of $\gamma\text{-Mn}_2\text{O}_3$ and manganese silicate, respectively. The FTIR spectra, though not useful because of the strong bands of the support that overlap those of manganese oxides, support these findings.

1 Introduction

Manganese oxides, both bulk and supported, have been employed as catalysts in the oxidation of carbon monoxide,^{1,2} hydrogen,² methanol,² hydrocarbons² and ammonia,³ in the decomposition of N_2O^4 and hydrogen peroxide,⁵ the selective reduction of nitric oxides,³ the hydrogenation of ethylene⁶ and the removal of hydrogen sulfide.⁷

Vibrational spectroscopies—Raman and IR—have proved valuable for the characterisation of surface molecular species of supported oxides that have a pronounced covalent character of the metal–oxygen bond, such as vanadium,⁸ molybdenum,⁹ tungsten¹⁰ and other oxides. Bulk manganese oxides were analysed using Raman spectroscopy in refs. 11–16 and IR in refs. 13, 17–21. Studies on the supported forms were fewer and were mainly carried out on oxides supported on alumina.^{11,12} A careful examination of the results published

earlier by different authors^{11,13,15} and of those that have more recently appeared^{12,14,16} shows discordance regarding the Raman spectra of manganese oxides. More reproducible results were obtained within IR studies. Examining the interaction of the support with the oxidic manganese phases, Kapteijn *et al.*¹² monitored the hydroxyl groups of alumina in the region 3600–3800 cm^{-1} to clarify the mechanism of Mn exchange on the surface of alumina, but they paid less attention to the region of 200–1200 cm^{-1} where the bands of the manganese oxides appear.

In this paper we attempt to investigate the possibilities and limits of Raman and IR spectroscopies as complementary techniques in the characterisation of bulk and supported (on Al_2O_3 and SiO_2) manganese oxides used as solid catalysts. To examine the local distribution of oxidic species on the support surface and its evolution with increasing amount of supported manganese oxides, the Raman technique was used in a microscopic configuration. The influence of the wavelength of the laser excitation on the Raman spectra was also studied. The Raman analysis is complemented by the characterisation of the oxides through X-ray diffraction and FTIR spectroscopy.

2 Experimental

MnO_2 was obtained from Merck (Braunstein). Mn_3O_4 was prepared from MnO_2 by calcination at 1273 K in air for 12 h,²² and Mn_2O_3 by heating $\text{Mn}(\text{NO}_3)_2 \cdot 4\text{H}_2\text{O}$ (Merck) in air at 923 K for 6 h.²³ The supported samples were prepared by pore volume impregnation of dried $\gamma\text{-Al}_2\text{O}_3$ (American Cyanamid, $S_{\text{BET}} = 200 \text{ m}^2 \text{ g}^{-1}$) and SiO_2 (Davidson Chem. Inc., $S_{\text{BET}} = 300 \text{ m}^2 \text{ g}^{-1}$) with an aqueous solution of $\text{Mn}(\text{NO}_3)_2$ of the appropriate concentration. The catalysts were then dried at 393 K (12 h) and heated in air at 773 K (6 h). The two series of supported manganese oxides were labelled MA*i* and MS*i*, where *i* indicates the manganese content expressed as number of atoms of manganese per 100 atoms of aluminium and silicon, respectively. The values of *i* are 0.05, 2, 6, 10, 14 and 18. The samples were then analysed on a Rigaku XRD diffractometer using $\text{Cu-K}\alpha$ ($\lambda = 0.15418 \text{ nm}$) radiation.

The Raman spectra were taken at room temperature in the spectral range 200–850 cm^{-1} using a Dilor XY Raman Spectrometer equipped with a CCD camera for multichannel detection and an optical microscope (objective 100 \times) that provided a laser beam focus diameter of about 1 μm . The spectra were taken using the 2.71 eV (457.9 nm) and 2.41 eV (514.5 nm) Ar^+ lines and the 1.92 eV (647.1 nm) Kr^+ line. The laser power in front of the microscope was 10 mW. The monochromator slits were set for a spectral resolution of 2 cm^{-1} . The time for spectral acquisition was 2 min and each spectrum was recorded three times, the average being taken. Pressed pellets were used as samples.

The FTIR measurements were performed at room temperature using a Bruker IFS66 spectrometer. Transmittance spectra at normal incidence were carried out over 350–2000 cm^{-1} using a DTGS detector. The samples were diluted in KBr.

3 Results and discussion

3.1 Raman spectra of bulk oxides

To study the influence of the wavelength of the incident radiation on the Raman response, spectra were taken at 10 mW power using violet (457.9 nm), green (514.5 nm) and red (647.1

† Present address: Department of Chemistry and Chemical Engineering, "Babes-Bolyai" University, 3400 Cluj-Napoca, Romania.

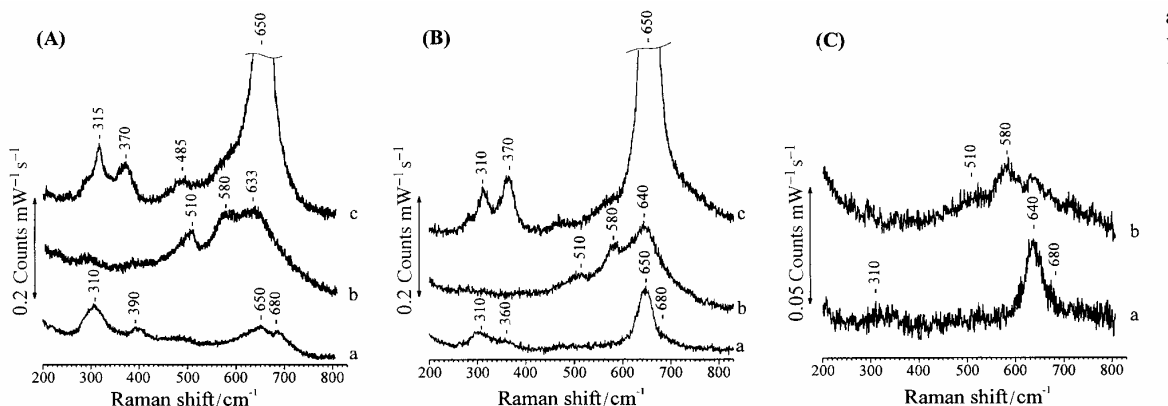


Fig. 1 Raman spectra of (a) Mn_2O_3 , (b) MnO_2 and (c) Mn_3O_4 recorded using $\lambda =$ (A) 647.1, (B) 514.5 and (C) 457.9 nm laser lines.

nm) laser light (Fig. 1). Under the microscope the beam was focused on the surface of well-grown crystallites of a few microns in diameter. As one can clearly see, the use of green and red exciting laser radiation gives the most intense spectra with the best resolution of Raman peaks (Fig. 1) and Mn_3O_4 has the most Raman intense modes of the three oxides. Its strongest peak at about 650 cm^{-1} and the two smaller peaks at $310\text{--}315$ and 370 cm^{-1} are in good agreement with the literature data.^{11,12,16} It also has a weaker signal at 485 cm^{-1} .

MnO_2 was not found to be Raman active by Strohmeier and Hercules¹¹ and Kapteijn *et al.*,¹² whereas Gosztola and Weaver¹⁴ and Bernard *et al.*¹⁶ reported well-defined spectra of this oxide. In our spectra of MnO_2 , three major features can be recognised: at $500\text{--}510$, $575\text{--}580$ and $630\text{--}640\text{ cm}^{-1}$. The band of $\sim 580\text{ cm}^{-1}$ was also observed in ref. 14 and was attributed to Mn—O lattice vibrations in MnO_2 . Among the signals of the MnO_2 Raman spectrum in ref. 16, the strongest lie at 523 , 576 , 633 and 650 cm^{-1} , the latter being assigned to Mn_3O_4 formed during the spectrum acquisition because of the local heating of the samples. In our spectra of MnO_2 a band was recorded at $630\text{--}640\text{ cm}^{-1}$ whose intensity is, however, extremely small compared with the Mn_3O_4 peak. The appearance of a 633 cm^{-1} band in the case of MnO_2 excited with a 50 mW laser power was explained in ref. 16 by the formation of a new XM compound which was identified as $\gamma\text{-Mn}_2\text{O}_3$ with a distorted hausmannite structure, an intermediate formed during the decomposition of MnO_2 to Mn_3O_4 . Therefore, the peaks at $ca.$ 510 and 580 cm^{-1} will be considered as the characteristic features of MnO_2 .

Mn_2O_3 gave a peak at $640\text{--}650\text{ cm}^{-1}$ (which is much greater in violet and green light than in red light) and a pair of features at $ca.$ 310 and $360\text{--}390\text{ cm}^{-1}$. We assume that these are owing to the formation of Mn_3O_4 during the spectra acquisition. Knowing that, as regards the oxidation state of the manganese ions, Mn_2O_3 is nearer to Mn_3O_4 than is MnO_2 , one can understand why Mn_2O_3 decomposes quicker and the features of Mn_3O_4 are more pronounced in its Raman spectrum. What we consider as characteristic for Mn_2O_3 is the peak at 680 cm^{-1} , which also appears in an earlier work¹³ as the main feature of this oxide. In ref. 12 the Mn_2O_3 spectrum, taken macroscopically, has three weak peaks at 311 , 653 and 697 cm^{-1} . Curiously there is no similarity between our Mn_2O_3 spectrum and that of ref. 16 where, except some differences between the relative peak heights, Mn_2O_3 has the same feature as MnO_2 .

Our results regarding the Raman frequencies of manganese oxides together with previous literature data are presented in Table 1.

3.2 Raman spectra of supported oxides

In earlier work, only Kapteijn *et al.* obtained spectra of manganese oxides supported on alumina¹² whereas Strohmeier and Hercules couldn't obtain any spectra for similar samples.¹¹ There are no Raman data regarding the manganese oxides supported on silicon oxide.

The spectra in ref. 12 recorded for alumina loaded with 2 to 8.4 wt.% Mn deposited from nitrate presented a broad peak at

Table 1 Raman frequencies of manganese oxides

Oxide	Raman shift/ cm^{-1}								Ref.
$\alpha\text{-Mn}_2\text{O}_3$	311 w					653 w		697 w	12
						620 w	672 s		13
	310 m ^b	360–390 w ^b	509 m	581 s	630 m ^a	650 w			16
$\gamma\text{-Mn}_2\text{O}_3$					650 s ^b	680 m			This work
$\beta\text{-MnO}_2$					633 s				16
	392 w		523 m	576 s	633 w ^a	650 m ^b			14
			510 w	580 m	633–640 w ^a				16
Mn_3O_4	319 w	374 w				.659 s			11
	316 w	368 w				654 s			12
	315 w	365 w				651 s			16
	310–315 w	370 w				650 s			This work
MnO			544 m			648 s			12
			537 s			645 w			15
			521 s	595 w					16

^{a,b} Attributed to the *in situ* formation of $\gamma\text{-Mn}_2\text{O}_3$ (a) and Mn_3O_4 (b) during spectrum acquisition.

about 650 cm^{-1} , characteristic of Mn_3O_4 . For the sample with 1 wt.% Mn from nitrate, as well as the samples with various concentrations of Mn deposited from acetate, this peak was found at about $637\text{--}647\text{ cm}^{-1}$. The authors attributed this shift to a higher dispersion of the manganese oxide, which gives rise to a new surface metal oxide phase. It may be suggested that this new phase could be $\gamma\text{-Mn}_2\text{O}_3$ whose formation is induced through the structure of the $\gamma\text{-Al}_2\text{O}_3$ used as support.²²

Using the microscopic configuration we took advantage of the possibility to analyse locally—within the focus diameter of $1\text{ }\mu\text{m}$ —the structure of the catalyst surface. During preliminary tests the green laser line led to the best spectra for supported oxides.

$\text{MnO}_x/\text{Al}_2\text{O}_3$ catalysts. The optical appearance of the catalysts is, especially for those with low manganese loading, highly inhomogeneous, with a rough white surface spotted with dark islands. Small crystallites appear here and there on the surface, having a dark or bright look. This inhomogeneity disappears as the Mn loading increases, the appearance of the catalyst turning to a dark, rough surface. The Raman spectra taken on different points of the surface for a low-loaded catalyst sample are presented in Fig. 2.

The difference in surface composition on going from one point to another is obvious. Not only the manganese oxide content varies from zero, in the white regions, to a very high amount for dark crystals, but also the oxide phase is different. The isolated crystal reveals the features of Mn_3O_4 , although the wings both on the left and on the right side of the peak at 650 cm^{-1} could be due to the peaks at 630 cm^{-1} (characteristic for $\gamma\text{-Mn}_2\text{O}_3$) and 680 cm^{-1} ($\alpha\text{-Mn}_2\text{O}_3$). In the case of point (c) in Fig. 2—the dark, rough islands on the surface—the shoulder at about 630 cm^{-1} can be well distinguished. It seems that, besides any Mn_3O_4 formed during spectrum acquisition, these islands consist of $\gamma\text{-Mn}_2\text{O}_3$ whose formation from the Mn precursor is induced by the $\gamma\text{-Al}_2\text{O}_3$ support. The feature at 750 cm^{-1} of the alumina support (Fig. 3) can also be recognised, showing that the Mn oxide layer is thin enough to allow the acquisition of the support spectrum, which was not the case for the crystal. Finally, point (b) in Fig. 2 (grey coloured) shows, besides the 630 and 650 cm^{-1} peaks

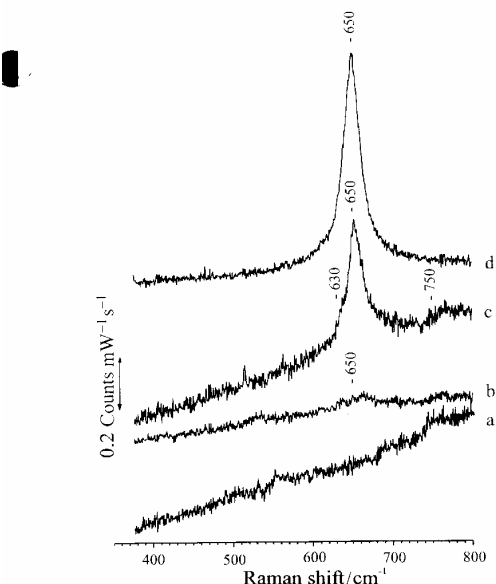


Fig. 2 Raman spectra taken at different points of the surface of alumina-supported catalyst MA2: (a) white point; (b) grey point; (c) dark point; and (d) dark crystal.

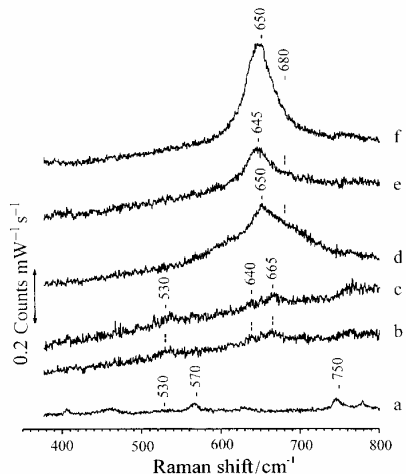


Fig. 3 Raman spectra of $\text{MnO}_x/\gamma\text{-Al}_2\text{O}_3$ series: (a) $\gamma\text{-Al}_2\text{O}_3$, (b) MA2, (c) MA6, (d) MA10, (e) MA14 and (f) MA18, taken at the rough surface.

of low intensity that are probably due to a decreased layer thickness, another weak feature at $530\text{--}540\text{ cm}^{-1}$. As this kind of signal did not appear in any of the spectra of pure Mn oxides obtained by us (and taking into account that among the values given in the literature for MnO Raman peaks a feature at 537 cm^{-1} is listed in ref. 15 and two features are given at 521 and 547 cm^{-1} in ref. 16) we assume that this peak is due to a $\text{Mn}^{II}\text{-O}$ vibration of isolated manganese ions “accommodated” superficially in the tetrahedral and/or octahedral vacancies of the alumina surface. This feature can be seen also in the spectra taken on the rough surface of the MA2 and MA6 catalysts (Fig. 3), and disappears for the high-loaded catalysts, probably owing to the increased thickness of the manganese oxide layer, which does not allow the signals from the support–oxide interface to be recorded. This is also confirmed by the disappearance of the alumina features at 570 and 750 cm^{-1} (Fig. 3).

The existence of Mn^{2+} in tetrahedral sites on the surface of $\gamma\text{-Al}_2\text{O}_3$ impregnated with manganese nitrate and heated at $600\text{ }^\circ\text{C}$ was demonstrated by Pott and McNicol using phosphorescence spectroscopy.²⁴ Moreover, the existence of isolated manganese cations on the surface of Al_2O_3 -supported manganese oxides deposited from acetate was observed in a recent study by Kijlstra *et al.*,²⁵ who showed that on catalysts containing less than 4.5 wt.% manganese the loaded metal was present as a mixture of Mn^{2+} , Mn^{3+} and Mn^{4+} cations isolated on the surface and octahedrally co-ordinated.

The spectra of the whole MA series, taken on the rough surface, are presented in Fig. 3. The formation of the MnO_x layer can be easily followed, beginning with the MA2 sample.

As the manganese content increases, the peak at 665 cm^{-1} probably shifts to 680 cm^{-1} where it can be observed as a shoulder, indicating the growth of $\alpha\text{-Mn}_2\text{O}_3$ as a well-defined crystalline phase. The XRD diagrams support this finding (Table 2). The peak at $630\text{--}640\text{ cm}^{-1}$, indicative of a very thin superficial epitaxial $\gamma\text{-Mn}_2\text{O}_3$ phase, becomes ever more obscured due to the growth of a thicker $\alpha\text{-Mn}_2\text{O}_3$ layer.

What appears to be unclear is the absence of the characteristic MnO_2 features, *e.g.* $510\text{--}520$ and $575\text{--}580\text{ cm}^{-1}$, although the $\beta\text{-MnO}_2$ phase was the main bulk manganese oxide phase detected by XRD measurements on the medium-loaded catalysts (Table 2). This peculiarity could be explained by the low Raman activity of MnO_2 , on the one hand, and by the close coincidence of the main MnO_2 feature (that at $575\text{--}580\text{ cm}^{-1}$) with the $\gamma\text{-Al}_2\text{O}_3$ peak at 570 cm^{-1} . The sensitivity of Raman analysis to the surface of the samples could be

Table 2 Manganese species identified by XRD and Raman at various manganese loadings on alumina and silica carriers

Samples	$\beta\text{-MnO}_2$		$\alpha\text{-Mn}_2\text{O}_3$		$\gamma\text{-Mn}_2\text{O}_3$		Mn_3O_4		MnO		Unknown phase	
	XRD	Raman	XRD	Raman	XRD	Raman	XRD	Raman	XRD	Raman	XRD	Raman
MA0.5	—	—	—	—	—	—	—	—	—	—	—	—
MA2	+	—	—	+	—	+	—	—	—	+	—	—
MA6	+	—	+	+	—	+	—	+	—	+	—	—
MA10	+	—	+	+	—	+	—	+	—	—	—	—
MA14	+	—	+	+	—	+	—	+	—	—	—	—
MA18	+	—	+	+	—	+	—	+	—	—	—	—
MS0.5	—	—	—	—	—	—	—	+	—	+	—	+
MS2	+	+	—	+	—	—	—	+	—	+	—	+
MS6	+	+	—	+	—	—	—	+	—	+	—	+
MS10	+	+	+	+	—	—	—	+	—	+	—	+
MS14	+	+	+	+	—	—	—	+	—	—	—	+
MS18	+	+	+	+	—	—	—	+	—	—	—	+

(+) Detected; (—) not detected.

another reason for the difference between the Raman and XRD analysis. The XRD diagrams reveal the presence of only bulk $\beta\text{-MnO}_2$ and $\alpha\text{-Mn}_2\text{O}_3$ phases, whereas the Raman spectra allow the identification of other surface manganese oxide species (Table 2).

MnO_x/SiO₂ catalysts. The MnO_x/SiO₂ spectra also show an obvious difference between those taken on the plain surface [Fig. 4(A)] and those taken on well-defined crystals [Fig. 4(B)]. In spectra taken on plain surface points, the characteristic feature of the SiO₂ support with a strong peak at about 490–500 cm⁻¹ can be easily recognised in the MS0.5–MS10 spectra, and disappears as the MnO_x layer increases for the MS14 and MS18 samples [Fig. 4(A)].

The XRD analysis fails to reveal, as in the case of MnO_x/alumina, any manganese oxide phase for MS0.5. Using Raman analysis it can be already detected on the plain surface but it is much more clearly seen on selected crystals on the surface [see Figs. 4(A) and 4(B)]. The peak at 530 cm⁻¹, attributed to isolated Mn²⁺ on the surface (a species which was also detected by Pott and McNicol for Mn²⁺/SiO₂, using phosphorescence spectroscopy,²⁴ and assigned as tetrahedrally co-ordinated) can be again observed, both for plain surface and crystals, except for the highest loaded samples. In our case the co-ordination of this cation should also be tetrahedral, as the cationic vacancies of the SiO₂ surface have a tetrahedral geometry. On this basis, together with the fact that the position of the corresponding Raman signal is the same both for the Al₂O₃ and the SiO₂ supported samples, we assume that the isolated Mn²⁺ ions on the surface of alumina are also tetrahedrally co-ordinated.

The features in the Raman spectra are, in the case of the MS series compared with the MA series, better defined and have more distinct line shapes. This could be owing to a better crystallisation of the MnO_x layer because of a weaker interaction with the SiO₂ support, on the one hand, and to a better reflectivity of the SiO₂ than that of Al₂O₃, giving a stronger Raman scattering. Unlike the MA series, the MS series gives very good MnO₂ features at 500–510 and 575 cm⁻¹, and the $\alpha\text{-Mn}_2\text{O}_3$ peak at 675 cm⁻¹ can be easily recognised as a shoulder of the stronger 650 cm⁻¹ signal owing to Mn₃O₄ formed under the laser beam.

Besides these features of known origin, a new well-defined peak appears in the MS spectra at 610–615 cm⁻¹. None of the manganese oxides characterised in the literature, as with our manganese oxides, gave such a signal, which leads us to consider it as a vibration due to a Mn—O—Si bonding. Whether this new Mn—Si—O phase existed already in the calcinated MS samples or it evolved only during the spectra acquisition due to the heating under the laser beam cannot yet be decided.

However, as the peak at 650 cm⁻¹, belonging to the Mn₃O₄ formed under the laser beam, decreases in the MS14 and MS18 spectra, whereas the 615 cm⁻¹ peak remains unchanged, we suppose that this Mn—Si—O phase already existed in the MnO_x/SiO₂ catalyst before Raman spectra acquisition. It is interesting that no such phase was identified by XRD measurements, indicating that this could be a

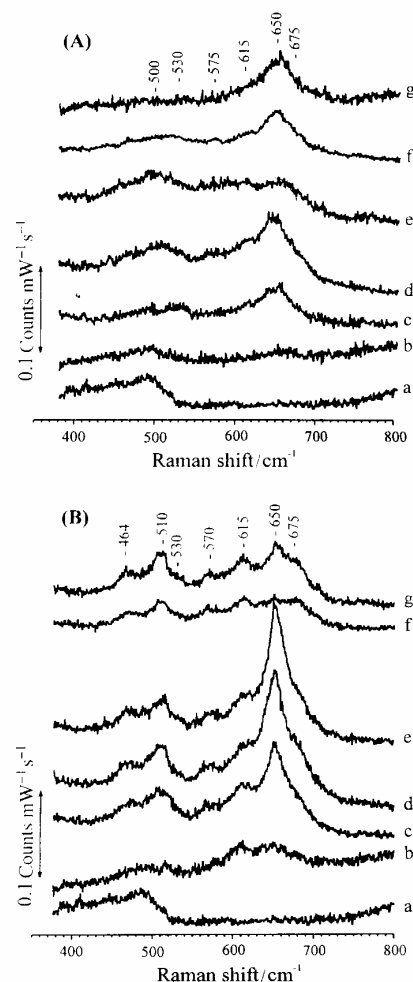


Fig. 4 Raman spectra of the MnO_x/SiO₂ series, taken at (A) the rough surface; (B) a well grown crystal on the surface: (a) SiO₂, (b) MS0.5, (c) MS2, (d) MS6, (e) MS10, (f) MS14 and (g) MS18.

Table 3 IR bands of pure manganese oxides

Oxide	Wavenumber/cm ⁻¹												Ref.
$\alpha\text{-Mn}_2\text{O}_3$	298	332	360	405	450	496	532	583	602	674			13
					370	410	450	496	525	580	600	670	19
$\gamma\text{-Mn}_2\text{O}_3$						480	520	580	600	670			This work
						470	520		600	650			18
$\beta\text{-MnO}_2$							530		600	660			18
							530		600	660			20
Mn_3O_4			370			465	530	590		720	850		This work
				352	412	502		612					17
					420	500		620					18
					430	500		610			960	1040	This work

“molecular” two-dimensional layer, epitaxially grown at the interface between the support and the MnO_x phases.

3.3 FTIR spectra

In the case of supported Mn oxides, the IR bands of the MnO_x species are strongly shadowed by those of the supports, which make their observation rather difficult. In addition, the very close bands of Mn_2O_3 and MnO_2 do not allow the discrimination of these species in the supported manganese oxides by means of IR spectra (Table 3).

In the MA series, besides the 530 and 570 cm⁻¹ bands that appear at higher manganese concentrations and can be attributed to the formation of well-defined MnO_2 and Mn_2O_3 phases, a new band appears at 610–620 cm⁻¹ and increases as the Mn concentration increases [Fig. 5(A)]. This band can be

seen also in the spectra of the MS series [Fig. 5(B)]. As in ref. 17 the band at 612 cm⁻¹ in the spectrum of Mn_3O_4 was assigned to Mn—O vibrations of bivalent manganese ions in tetrahedral co-ordination, one can suppose that the presence of this feature in the spectra of supported manganese oxide arises from the isolated Mn^{2+} ions accommodated in the tetrahedral vacancies of the support surface. Another striking feature of the MS spectra is the enhancement of the band at 1100 cm⁻¹ relative to the shoulder at 1200 cm⁻¹, which could be owing to a superimposing of a Mn—O—Si vibration that arises from the bidimensional layer at the interface between SiO_2 and MnO_x .

4 Conclusions

The use of Raman spectroscopy for the characterisation of surface species in the supported manganese oxides has rarely been used so far. The main difficulties are the insufficient data about the bulk oxides themselves, owing to a pronounced instability under the laser beam which render the acquisition of “pure” spectra difficult, on the one hand, and the weak Raman activity of the manganese oxides which causes poor results in case of macroscopic measurements.

As Raman spectroscopy is envisaged to be a characterisation method for surface species, the use of the microscopic laser excitation which is confined to a narrow area of the surface and, by using a low laser-power, to a thinner layer in the neighbourhood of the surface appears to be a more suitable method to achieve this purpose. The spectra obtained in this way are better defined and it is also possible to study the correlation between the optical aspect of the catalyst surface, as it appears in the microscope, and the phase composition of the various points on the surface. Raman spectroscopy also allows the identification of two-dimensional manganese species formed at the interface between the support and the manganese oxide layer, which are invisible in XRD.

The use of FTIR spectroscopy for identification of manganese species formed on the surface of alumina and silica is hindered by the bands of the supports themselves. However, the existence of some bands which do not appear in the spectra of pure oxides support the formation of the new “molecular” manganese species assigned on the basis of Raman spectra.

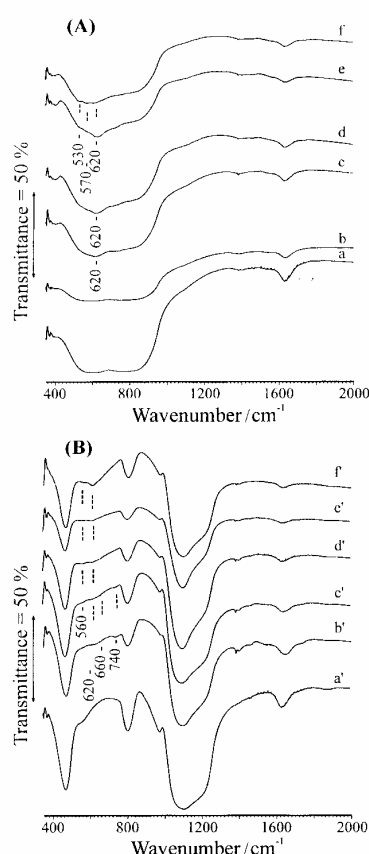


Fig. 5 FTIR spectra of (A) $\text{MnO}_x/\gamma\text{-Al}_2\text{O}_3$ -series; (B) $\text{MnO}_x/\text{SiO}_2$ -series: (a) $\gamma\text{-Al}_2\text{O}_3$, (b) MA2, (c) MA6, (d) MA10, (e) MA14 and (f) MA18; (a') SiO_2 , (b') MS2, (c') MS6, (d') MS10, (e') MS14 and (f') MS18.

References

- S. B. Kanungo, *J. Catal.*, 1979, **58**, 419.
- G. K. Boreskov, in *Catalysis Science and Technology*, ed. J. R. Anderson and M. Boudart, Akademie Verlag, Berlin, 1983, p. 83, 108, 118.
- L. S. Singoredjo, R. B. Korver, F. Kapteijn and J. A. Moulijn, *Appl. Catal. B: Environ.*, 1992, **1**, 297.
- M. Lo Jacono and M. Schiavello, in *Preparation of Catalysts*, ed. B. Delmon, D. A. Jacobs and G. Poncelet, Elsevier, Amsterdam, 1976, p. 474.